

UDC 541.6:541.49:546.74

DFT STUDIES ON THE TETRANUCLEAR CUBANE COMPLEX $[\text{Ni}_4(\text{ampd})_4(\text{Cl}_4)] \cdot \text{MeCN}$

G. Abbas¹, Mariya-al-Rashida², A. Irfan³, U. Ali Rana⁴, I. Shakir⁴

¹*Interdisciplinary Research Centre in Biomedical Materials, COMSATS Institute of Information Technology Lahore, Pakistan*

E-mail: abbas191@gmail.com

²*Department of Chemistry, Forman Christian College University, Lahore, Pakistan*

E-mail: mariya-al-rashida83@yahoo.com

³*Department of Chemistry, Faculty of Science, King Khalid University, Abha, Saudi Arabia*

E-mail: irfaahmad@gmail.com

⁴*Deanship of Scientific Research, College of Engendering, King Sand university, Riyadh, Saudi Arabia*

E-mail: ranausmanali4u@gmail.com, Imranskku@gmail.com

Received September, 23, 2012

Revised — January, 15, 2013

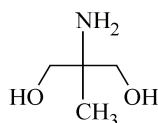
Density functional theory (DFT) is used to investigate the structural properties of Ni(III) cubane $[\text{Ni}_4(\text{ampd})_4(\text{Cl}_4)] \cdot \text{MeCN}$. The structural features and ground state geometry calculations are computed at the B3LYP/6-31G* (LANL2DZ) level of theory. We shed light on the highest occupied molecular orbital and lowest unoccupied molecular orbital. The absorption spectrum is calculated using time-dependent DFT. The absorption wavelengths are calculated using different functionals, i.e., pw91pw91, B3LYP, BHandHLYP, CAM-B3LYP, LC-BLYP, and M06. The LC-BLYP is in good agreement with the experimental data.

К e y w o r d s: Ni(II) cubane, 2-amino-2-methyl-2,3-propandiol, single crystal X-ray crystallography, density functional theory, time-dependent density functional theory.

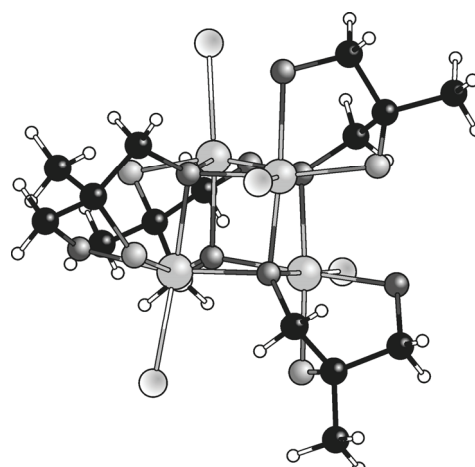
INTRODUCTION

The synthesis of polynuclear metal complexes has attracted immense interest in the last two decades [1]. The high nuclearity nickel aggregates possess aesthetically pleasing structures and are also relevant to many important fields, including bioinorganic chemistry and molecular magnetic materials. In the former field, the synthesis and characterization of nickel(II) hydroxo-bridged dimers is important since such species provide useful bioinorganic models for the intermediates in the catalytic mechanism of the metalloenzyme urease [2]. Similar clusters have sparked interest among scientists for their potential applications as biomimetic agents to study the enzyme catalysis [3—6]. More pronounced applications of polynuclear clusters of paramagnetic metals include their role as single molecule magnets (SMMs). The last decade has seen an explosion in the field of SMM research. One of the earliest molecules to be identified as SMMs were manganese oxide based clusters [7], however, many more iron [8], cobalt [9], and nickel [10] based SMMs have since been developed. What makes these molecules even more interesting is the phenomena of magnetic hysteresis, a property that offers much hope for the application of these materials as storage devices or qubits (quantum bits), providing impetus to push research in the direction of spintronics (spin based molecular electronic devices) [11]. Such materials are also strong candidates for the use in cooling applications owing to the presence of the enhanced magnetocaloric effect (MCE) [12].

The first nickel based SMM was a cyclic dodecanuclear complex [13]. One successful synthetic methodology towards new Ni^{II} compounds includes the employment of ligands that contain RO-

Scheme 1. Structure of the ampdH₂ ligand

groups since they have a high bridging capability, thus leading to polynuclear compounds and often propagateing ferromagnetic interactions between the metal centers [11]. Some of the more commonly investigated RO-containing ligands include hmpH (2-hydroxymethylpyridine), thmeH₃ (1,1,1-tris(hydroxymethyl)ethane), pdmH₂ (pyridine-2,6-dimethanol) and metheidiH₃ (N-(1-hydroxymethyl-ethyl)iminodiacetic acid) [11]. We have already reported di- and tetranuclear lanthanide complexes obtained with the use of *N*-methyldiethanolamine and 2-amino-2-methyl-1,3-propandiol [14]. Few polynuclear complexes from this ligand have been reported to date, including a ferromagnetic decametallic mixed valent Mn supertetrahedron [15, 16], a mixed valent cobalt cluster [17], multinuclear Fe [18], Ni, and Co complexes [19]. Herein we report the DFT studies of a Ni cubane-like complex having the formula [Ni₄(ampd)₄(Cl₄)]_n·MeCN, which we prepared with minor modifications of the already known method [19]. The crystal structure of the compound has been determined with single crystal X-ray crystallography (Fig. 1). These crystal coordinates were then used to define the initial atomic coordinates in the computational analysis. Using DFT and time-dependent DFT, we have shed light on the geometries, electronic and optical properties respectively.

Fig. 1. Molecular structure of tetranuclear Ni(II) cubane [Ni₄(ampd)₄(Cl₄)]_n·MeCN with solvent molecules removed

EXPERIMENTAL

General and physical measurements. All chemicals and solvents used for the synthesis were obtained from commercial sources and were used as received, without further purification. The reaction was carried out under aerobic conditions. The compound was characterised by elemental analysis (CHN) using an Elementar Vario EL analyzer. Fourier transform IR spectra were measured on a Perkin-Elmer Spectrum.

Preparation of [Ni₄(ampd)₄(Cl₄)]_n·MeCN (1·MeCN). A solution of 2-amino-2-methyl-1,3-propandiol (0.079 g, 0.75 mmol) in MeCN (15 ml) was added dropwise over 20 min to a stirred solution of NiCl₂·6H₂O (0.119 g, 0.5 mmol) in MeOH (15 ml). The resulting mixture was stirred at room temperature (RT) for 2 h, filtered, and allowed to stand undisturbed in a sealed vial. Green coloured rods suitable for the single crystal X-ray diffraction analysis were obtained after 3 weeks. A part of the crystals was maintained in the mother liquor for X-ray crystallography and another part of them was collected by filtration, washed with MeCN and dried in vacuum. Yield: 45 %. Anal. Calcd (found) for C₁₆H₃₂Cl₄N₄O₈: C 24.479 (24.356), H 4.108(3.986), N 7.136—(6.973) %. IR (KBr): ν (cm⁻¹) = 3423 (w), 2960 (s), 2927 (w), 2867 (w), 1683 (vs) 1566 (s), 1431 (s), 1376 (m), 1361 (m), 1320 (w), 1327 (m), 1228 (s), 1151 (w), 1137 (w), 1086 (w), 1077 (w), 1046 (w), 971 (w), 938 (w), 897 (m), 808 (m), 792 (m), 776 (w), 608 (m), 559 (w), 468 (w).

X-ray crystallographic studies. Data were collected on an Oxford-Diffractometer equipped with a CCD area detector and a graphite monochromator utilizing MoK_α radiation ($\lambda = 0.71073 \text{ \AA}$). A greenish suitable crystal was attached to glass fibers using paratone-N oil and transferred to a goniostat where it was cooled for data collection. Unit cell dimensions were determined and refined using 3823 ($2.94 \leq \theta \leq 28.80^\circ$) reflections. Empirical absorption correction (multi-scan based on symmetry-related measurements) were applied using the CrysAlis RED software [20]. The struc-

ture was solved by direct methods using SIR92 [21] and refined on F^2 using full-matrix least squares with SHELXL97 [22]. Programs used: CrysAlis CCD [20] for data collection, CrysAlis RED [20] for cell refinement and data reduction, and DIAMOND [23] for molecular graphics. The non-H atoms were treated anisotropically, whereas the hydrogen atoms were placed in calculated, ideal positions and refined as riding on their respective carbon atoms. Full details can be found in the CIF files deposited with the Cambridge Crystallographic Data Center, CCDC No. 879548. The structure contains severely disordered lattice solvent molecules (CH_3CN , MeOH , H_2O) that could not be modeled properly; thus the SQUEEZE program, a part of the PLATON package of the crystallographic software, was used to calculate the solvent disorder area and remove its contribution from the intensity data [24].

COMPUTATIONAL METHODOLOGY

The computations of the geometries and electronic structures were performed using DFT with the Gaussian 09 package [25]. DFT was treated according to Becke's three parameter gradient-corrected exchange potential and the Lee-Yang-Parr gradient-corrected correlation potential (B3LYP) [26–28], and all calculations were performed using the 6-31G* basis set [29], and the LANL2DZ basis set, which was found to be precise for metal containing systems, was applied for Ni [30—34]. The structures investigated in the present study were optimized in the ground state (S_0) at the B3LYP/6-31G* (LANL2DZ) level of theory. Absorption spectra were calculated using time-dependent DFT. At the first step we have computed the absorption wavelengths at NStates = 3 at different level of theories and checked the effect of different functionals (exchange functional, correlation functionals, hybrid functional, and long-range corrected functionals) on the absorption wavelengths, i.e., pw91pw91 [35], B3LYP [36, 37], BHandHLYP [38], CAM-B3LYP [39], LC-BLYP [40], and M06 [41]. The LANL2DZ core potential was used for Ni metal while the 6-31G* basis set was used for C, N, O. All the functionals overestimate the experimental absorption wavelength. Among all functionals LC-BLYP gave the closest value to the experimental data. Thus, at the next step, we have computed the absorption spectrum using ten NStates at the LC-BLYP/6-31G* level of theory. The absorption wavelength computed at this level of theory is in good agreement with the experimental evidence. The density of states (DOS) and the UV-visible spectrum of these systems were convoluted using the Gauss-Sum 2.1 and Chemcraft softwares respectively [42—44].

RESULTS AND DISCUSSION

The structure of **1** was determined by single-crystal X-ray diffraction. The molecular structure is essentially the same as that reported earlier [19], however, there is a difference in the nature of solvent molecules present in the crystal lattice. For the purpose of the DFT analysis the initial atomic coordinates were selected from the crystal analyzed by us (and therefore reported here). The compound crystallized in the monoclinic space group $P2_1/n$ with $Z = 2$. The crystal structure of **1** showed a discrete cubane-like tetranuclear molecule $[\text{Ni}_4(\text{ampd})_4(\text{Cl}_4)] \cdot \text{MeCN}$ (Fig. 2).

Geometries and electronic properties. The geometrical parameters, bond lengths, bond angles, dihedral angles as well as the dipole moment have been presented in Table 1. It can be seen that the

Table 1

Bond lengths (Å), bond angles, and dihedral angles (deg.) of the ground states at the B3LYP/6-31G(LANL2DZ) level of theory*

Parameter	Bond length		Parameter	Bond length		Parameter	Bond angles		Parameter	Torsion Angle	
	Opt	exp		Opt	exp		Opt	exp		Opt	exp
Ni1—Cl5	2.218	2.393	Ni1—O9	1.893	2.140	O14—Ni1—Cl5	91.56	97.02	Cl5—Ni1—Ni4—O15	4.91	6.12
Ni2—Cl6	2.197	2.346	Ni1—O14	2.020	2.067	O8—Ni4—Cl8	91.66	94.41	Ni1—Ni2—N3—Ni4	68.07	70.54
Ni3—Cl7	2.210	2.367	Ni1—N17	1.981	2.074	O14—Ni3—Cl7	175.92	177.44			
Ni1—Cl5	2.242	2.367	Dipole moment	1.141							

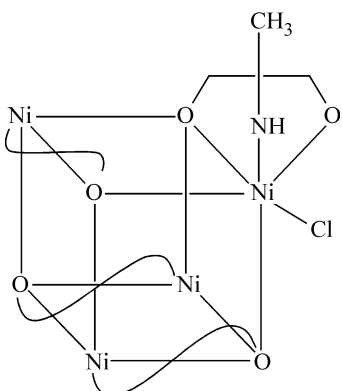


Fig. 2. $[\text{Ni}_4(\text{ampd})_4(\text{Cl}_4)] \cdot \text{MeCN}$ molecule.

Each Ni atom in the cubane-like core is coordinated to the tridentate ampd ligand and a chloride ion. These contacts are expanded for one Ni atom only on the top right side of the figure; on the other three sides these are represented as curved lines

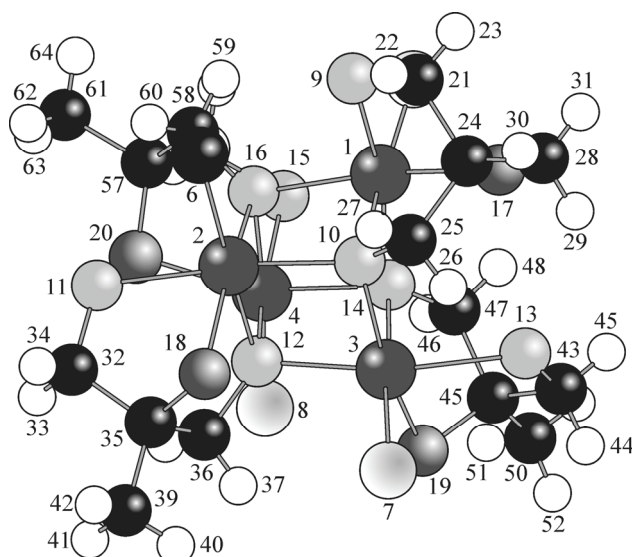


Fig. 3. Optimized structure of compound 1 at the B3LYP/6-31G*(LANL2DZ) level of theory

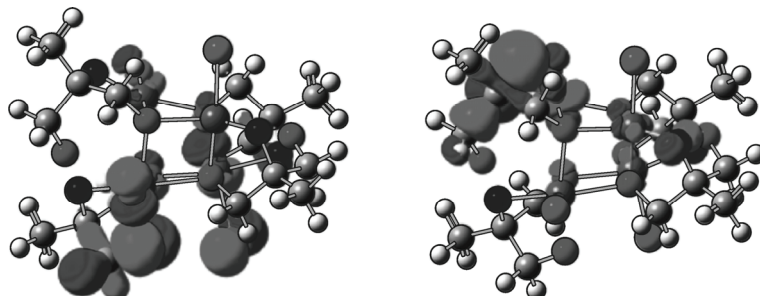


Fig. 4. Representations of the HOMO (left) and LUMO (right) orbital density of compound 1 at the B3LYP/6-31G*(LANL2DZ) level of theory

optimized geometrical parameters are in good agreement with the crystal structure parameters (atom numbering scheme in Fig. 3). The calculated dipole moment is 1.141.

Fig. 4 illustrates the calculated pattern of the highest occupied molecular orbitals (HOMOs) and lowest unoccupied molecular orbitals (LUMOs). The HOMO is localized on the lower left ligand; Cl atoms also make a contribution to the formation of HOMO; O_9 and O_{15} also take part in the pattern of HOMO. A very small contribution for Ni has been observed in the construction of HOMO. The LUMO is of the antibonding character with π^* distributed on the left top ligand; Ni_2O_{10} , N_{17} , and N_{63} take part in the development of LUMO as well. The HOMO-LUMO energy gap of this compound was calculated at the B3LYP/6-31G* (LANL2DZ) level of theory. The orbital energy level analysis at this level showed the HOMO energy (E_{HOMO}), LUMO energy (E_{LUMO}) and HOMO—LUMO energy gap (E_{gap}) of -6.69 eV, -4.92 eV, and 1.77 eV respectively.

In diverse physical systems DOS plays an imperative role. In Fig. 5, HOMO and LUMO are shown by green and blue lines respectively. The region between the green and blue lines demonstrates the energy gap. The energy of HOMO-1 MO is -6.46 eV. It is close to the HOMO energy. Fig. 5 illustrates that the electron occupancy is higher in HOMO than in LUMO, and the energy gap (1.77) revealed that it would be easy to transfer the electron from HOMO to LUMO. The energy difference between HOMO and HOMO-1 is diminutive. As we go from HOMO-4 to HOMO-12, the electron occupancy increases. The energy difference between LUMO and LUMO+1 is so small that both molecular orbitals emerged. There is a small difference in the energy of LUMO+3 to LUMO+10 while

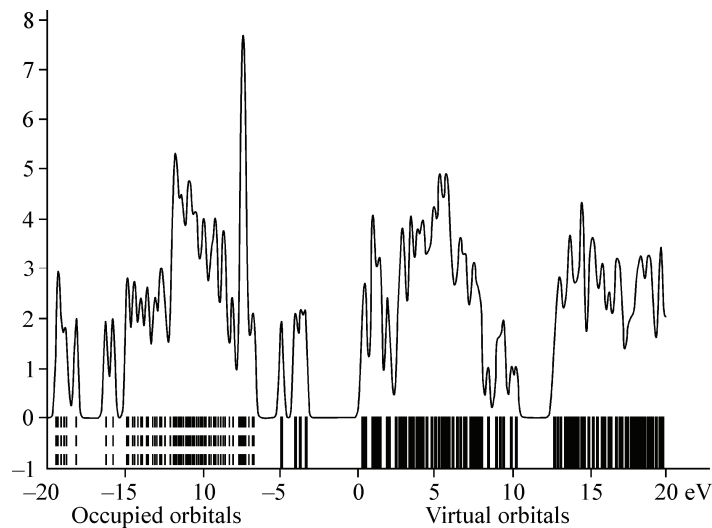


Fig. 5. DOS computed at the B3LYP/6-31G* (LANL2DZ) level of theory

the energy gap between LUMO+10 to LUMO+11 is more than twice the HOMO-LUMO energy gap, which revealed that it would be more difficult to transfer the electron from LUMO to LUMO+11, LUMO+12 and LUMO+13, etc.

Absorption spectrum. The computed absorption wavelengths at different level of theories are as follows: pw91pw91/6-31G* (LANL2DZ) (2886 nm), pw91pw91/6-31G* (LANL2DZ) (825 nm) BHandHLYP/6-31G* (LANL2DZ) (853 nm), CAM-B3LYP/6-31G* (LANL2DZ) (856 nm), LC-BLYP/6-31G* (LANL2DZ) (796 nm), and M06/6-31G* (LANL2DZ) (1343) using three NStates. All of the functionals overestimate the absorption wavelength. Among all functionals LC-BLYP is good because it less overestimates the experimental value. Then we computed the absorption spectrum at the LC-BLYP/6-31G* (LANL2DZ) level of theory. The calculated maximum absorption wavelength of 585 nm is in reasonable agreement with the experimental data of 652 nm (see the supporting information). The absorption spectrum of compound **1** has been presented in Fig. 6 at the LC-BLYP/6-31G* (LANL2DZ) level of theory. Moreover, two more peaks have also been observed at 755 nm and 795 nm respectively.

CONCLUSIONS

DFT studies were carried out for the tetranuclear $[\text{Ni}_4(\text{ampd})_4(\text{Cl}_4)] \cdot \text{MeCN}$ compound containing a Ni_4O_4 cubane-like core. Ground state geometry calculations were made at the DFT-B3LYP/6-31G* (LANL2DZ) level of theory. HOMO is localized on the lower left ligand, while LUMO is of the anti-bonding character with π^* distributed on the left top ligand. The energy gap between LUMO+10 to LUMO+11 is more than twice the HOMO—LUMO energy gap. The effect of functionals on the absorption spectrum was computed using time dependent DFT. The best functional to reproduce the experimental absorption data is LC-BLYP. Thus, it is esteemed that the LC-BLYP functional would be better to predict the absorption wavelengths of the tetranuclear cubane-type complex.

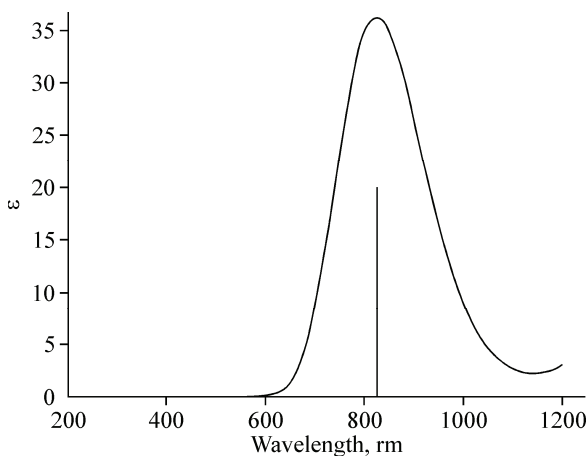


Fig. 6. Absorption spectrum of compound **1** computed at the TD-LC-BLYP/6-31G* (LANL2DZ) level of theory (top) and experimental one (bottom)

Acknowledgements. The authors are grateful to the COMSATS Institute of Information Technology, Islamabad, Pakistan for financial support and further author would like to extend their sincere appreciation to the Deanship of Scientific Research (DSR) at King Saud University for the funding of this research through the Research Group Project no RGP-VPP-312.

Supplementary material. Crystallographic data (excluding structure factors) for the structure reported in this paper have been deposited with the Cambridge Crystallographic Data Center, CCDC No. 879548. Copies of the data can be obtained free of charge on application to The Director, CCDC, 12 Union Road, Cambridge CB2 1EZ, UK, fax: +44 1223 336033, e-mail: deposit@ccdc.cam.ac.uk or <http://www.ccdc.cam.ac.uk>.

REFERENCES

1. *Sauvage J.P.* Transition Metals in Supramolecular Chemistry., vol 5 of Perspectives in Supramolecular Chemistry. – New York: Wiley., 1999.
2. *Wages H.E., Taft K.L., Lippard S.J.* // Inorg. Chem. – 1993. – **32**. – P. 4985 – 4987.
3. a) *Yang E.C., Wernsdorfer W., Zakharov L.N., Karaki Y., Yamaguchi A., Isidro R.M., Lu G.D., Wilson S.A., Rheingold A.L., Ishimoto H., Hendrickson D.N.* // Inorg. Chem. – 2006. – **45**. – P. 529. b) *Jiang L., Choi H.J., Feng X.L., Lu T.B., Long J.R.* // Inorg. Chem. – 2007. – **46**. – P. 2181. c) *Lillo J.M., Armentano D., Munno G.D., Wernsdorfer W., Julve M., Loret F., Faus J.* // J. Amer. Chem. Soc. – 2006. – **128**. – P. 14218. d) *Gregory C., Reto B., Ulrich G.H., Stefan O., Andrew P., Simon P., Gopalan R., Andreas S., Andrew S., Grigore T., Winpenny R.E.P.* // Dalton. Trans. – 2004. – P. 2758. e) *Heath S.L., Laye R.H., Muryn C.A., Lima N., Sessoli R., Shaw R., Teat S.J., Timco G.A., Winpenny R.E.P.* // Angew. Chem. Int. Ed. – 2004. – **43**. – P. 6132. f) *Aromi G., Batsanov A.S., Christian P., Helliwell M., Roubeau O., Timco G.A., Winpenny R.E.P.* // Dalton. Trans. – 2003. – P. 4466. g) *Canovas M.M., Helliwell M., Richard L., Riviere E., Wernsdorfer W., Brechin E.K., Mallah T.* // Eur. J. Inorg. Chem. – 2004. – P. 2219. h) *Brechin E.K.* // Chem. Commun. – 2005. – P. 5141.
4. a) *Karplus P.A., Pearson M.A., Hausinger R.P.* // Acc. Chem. Res. – 1997. – **30**. – P. 330. b) *Jabri E., Carr M.B., Hausinger R.P., Karplus P.A.* // Science. – 1995. – **268**. – P. 998. c) *Holm R.H., Kennepohl P., Solomon E.I.* // Chem. Rev. – 1996. – **96**. – P. 2239.
5. a) *Carlsson H., Haukka M., Nordlander E.* // Inorg. Chem. – 2002. – **41**. – P. 4981. b) *Mohanta S., Nanda K.K., Werner R., Haase W., Mukherjee A.K., Dutta S.K., Nag K.* // Inorg. Chem. – 1997. – **36**. – P. 4656. c) *Matthews C.J., Avery K., Xu Z., Thompson L.K., Zhao L., Miller D.O., Zaworotko M.J., Biradha K., Poirier K., Wilson C., Goeta A.E., Howard J.A.K.* // Inorg. Chem. – 1999. – **38**. – P. 5266. d) *Carlsson H., Haukka M., Bousseksou A., Latour J.M., Nordlander E.* // Inorg. Chem. – 2004. – **43**. – P. 8252. e) *Hahn F.E., Ochs C., Lugger T., Frohlich R.* // Inorg. Chem. – 2004. – **43**. – P. 6101.
6. a) *Peristeraki T., Samios M., Siczek M., Lis T., Milios C.J.* // Inorg. Chem. – 2011. – **50**. – P. 5175. b) *Baltazar C.S.A., Marques M.C., Soares C.M., DeLacey A.M., Pereira I.A.C., Matias P.M.* // Eur. J. Inorg. Chem. – 2011. – **7**. – P. 948. c) *Begum A., Moula G., Sarkar G.S.* // Chem. Eur. J. – 2010. – **16**. – P. 1232. d) *Barton B.E., Rauchfuss T.B.* // J. Amer. Chem. Soc. – 2010. – **132**. – P. 14877. e) *Cvetkovic A., Menon A.L., Thorgersen M.P., Scott J.W., Poole F.L., Jenney F.E., Lancaster W.A., Adams M.W.W.* // Nature. – 2010. – **466**. – P. 779.
7. *Sessoli R., Tsai H.L., Schake A.R., Wang S., Vincent J.B., Folting K., Gatteschi D., Christou G., Hendrickson D.N.* // J. Amer. Chem. Soc. – 1993. – **115**. – P. 1804.
8. *Delfs C., Gatteschi D., Pardi L., Sessoli R., Wieghardt K., Hanke D.* // Inorg. Chem. – 1993. – **32**. – P. 3099.
9. a) *Brechin E.K., Cador O., Caneschi A., Cadiou C., Harris S.G., Parsons S., Vonci M., Winpenny R.E.P.* // Chem. Commun. – 2002. – P. 1860 – 1861. b) *Cadiou C., Graham A., Harrison A., Helliwell M., Parsons S., Winpenny R.E.P.* // Chem. Commun. – 2002. – P. 1106 – 1107.
10. a) *Andres H., Basler R., Blake A.J., Cadiou C., Chaboussant G., Grant C.M., Gudel H.U., Murrie M., Parsons S., Paulsen C., Semadini F., Villar V., Wernsdorfer W., Winpenny R.E.P.* // Chem. Eur. J. – 2002. – **8**. – P. 4867. b) *Cadiou C., Murrie M., Paulsen C., Villar V., Wernsdorfer W., Winpenny R.E.P.* // Chem. Comm. – 2001. – P. 2666. c) *Dearden A.L., Parsons S., Winpenny R.E.P.* // Angew. Chem. Int. Ed. – 2001. – **40**. – P. 151.
11. *Jeffrey R.L.* In: Yang P. ed.) Molecular Cluster Magnets in Chemistry of Nanostructured Materials. – Hong Kong: World Scientific Publishing, 2003.
12. *Manoli M., Collins A., Parsons S., Candini A., Evangelisti M., Brechin E.K.* // J. Amer. Chem. Soc. – 2008. – **130**. – P. 11129.
13. *Cadiou C., Murrie M., Paulsen C., Villar V., Wernsdorfer R., Winpenny W.E.P., Abbas G., Lan Y., Kostakis G.E., Wernsdorfer W., Anson C.E., Powell A.K.* // Inorg. Chem. – 2010. – **49**. – P. 8067.

14. a) *Abbas G., Lan Y., Kostakis G., Anson C.E., Powell A.K.* // Inorg. Chim. Acta. – 2008. – **361**. – P. 3494.
b) *Abbas G., Kostakis G.E., Lan Y., Powell A.K.* // Polyhedron. – 2012. – **41**. – P. 1.
15. *Foguet-Albiol D., Abboud K., Christou G.* // Chem. Commun. – 2005. – **34**. – P. 4282.
16. *Manoli M., Johnstone R.D.L., Parsons S., Murrie M., Affronte M., Evangelisti M.E., Brechin K.* // Angew. Chem. Int. Ed. – 2007. – **46**. – P. 4456.
17. *Alley K.G., Bircher R., Waldmann O., Ochsenbein S.T., Güdel H.U., Moubaraki B., Murray K.S., Alonso F.F., Abrahams B.F., Boskovic C.* // Inorg. Chem. – 2006. – **45**. – P. 8950.
18. *Labat G., Boskovic C., Güdel H.U.* // Acta Crystallogr. – 2005. – **E61**. – P. m611.
19. *Alley K.G., Bircher R., Gudel H.U., Moubaraki B., Murray K.S., Abrahams B.F., Boskovic C.* // Polyhedron. – 2007. – **26**. – P. 369.
20. A multipurpose crystallographic tool. – Utrecht University: The Oxford Diffraction CrysAlis CCD and CrysAlis RED., version p171.33.34d., Oxford Diffraction Ltd., Abingdon., Oxford., England, 2009.
21. *Altomare A., Cascarano G., Giacovazzo C., Guagliardi A., Burla M.C., Polidori G., Camalli M.* // J. Appl. Crystallogr. – 1994. – **27**. – P. 435.
22. *Sheldrick G.M.* SHELXL97 University of Göttingen., Germany.
23. *Brandenburg K.* DIAMOND Crystal Impact GbR., Bonn., Germany, 1999.
24. a) *Spek A.L.* PLATON. Netherlands, 2003. b) SQUEEZE: van der Sluis P., Spek A.L. // Acta Crystallogr. Sect. A. – 1990. – **46**. – P. 194.
25. *Frisch M.J. et al.* Gaussian 09 Revision A.1 Gaussian Inc. Wallingford., CT, 2009.
26. *Becke A.D.* // J. Chem. Phys. – 1993. – **98**. – P. 5648.
27. *Miehlich B., Savin A., Stoll H., Preuss H.* // Chem. Phys. Lett. – 1989. – **157**. – P. 200.
28. *Lee C., Yang W., Parr R.G.* // Phys. Rev. B. – 1988. – **37**. – P. 785.
29. *Sun J., Song J., Zhao Y., Liang W.Z.* // J. Chem. Phys. – 2007. – **127**. – P. 234107.
30. *Wan L., Zhang Y.X., Qi D.D., Jiang J.H.* // J. Mol. Graphics. Modell. – 2010. – **28**. – P. 842.
31. *Liu Z.Q., Chen Z.X., Jin B.B., Zhang X.X.* // Vib. Spectrosc. – 2011. – **56**. – P. 210.
32. *Li L., Tang Q., Li H., Yang X., Hu W., Song Y., Shuai Z., Xu W., Liu Y., Zhu D.* // Adv. Mater. – 2007. – **19**. – P. 2613.
33. *Irfan A., Zhang J., Chang Y.* // Chem. Phys. Lett. – 2009. – **483**. – P. 143.
34. *Ma R., Guo P., Yang L., Guo L., Zeng Q., Liu G., Zhang X.* // J. Mol. Struct. (THEOCHEM). – 2010. – **942**. – P. 131.
35. *Burke K., Perdew J.P., Wang Y.* In Electronic Density Functional Theory: Recent Progress and New Directions. / Ed. J.F. Dobson, G. Vignale, M.P. Das. (Plenum., 1998).
36. *Walsh P.J., Gordon K.C., Officer D.L., Campbell W.M.* // J. Mol. Struct. (THEOCHEM). – 2006. – **759**. – P. 17 – 24.
37. *Cleland D.M., Gordon K.C., Officer D.L., Wagner P., Walsh P.J.* // Spectrochim. Acta. Part. A. – 2009. – **74**. – P. 931.
38. *Becke A.D.* // J. Chem. Phys. – 1993. – **98**. – P. 1372 – 77.
39. *Yanai T., Tew D., Handy N.* // Chem. Phys. Lett. – 2004. – **393**. – P. 51 – 57.
40. *Iikura H., Tsuneda T., Yanai T., Hirao K.* // J. Chem. Phys. – 2001. – **115**. – P. 3540 – 44.
41. *Zhao Y., Truhlar D.G.* // Theor Chem Acc. – 2008. – **120**. – P. 215 – 41.
42. *O'Boyle N.M., Tenderholt A.L., Langner K.M.* cclib: A library for package-independent computational chemistry algorithms. // J. Comp. Chem. – 2008. – **29**. – P. 839 – 845.
43. *Irfan A., Ijaz F., Al-Sehemi A.G., Asiri A.M.* // J. Comput. Electron. – 2012. – DOI 10.1007/s10825-012-0417-8
44. *Al-Sehemi A.G., Al-Amri R.S.A., Irfan A.* // Acta. Phys. Chim. Sin. – 2013. – **29**. – P. 1 – 9.